ADVANCED CONTROL SYSTEM FOR PHOTOVOLTAIC POWER GENERATION, STORAGE AND CONSUMPTION

Cristian MIRON[1], Severus OLTEANU[2], Nicolai CHRISTOV[3], Dumitru POPESCU[4]

This paper deals with the implementation of a system architecture for a photovoltaic (PV) module, assuring regulated voltage output at the consumer, maximum power point tracking (MPPT) as well as controlled storage of surplus energy. The usefulness of developing a simple to implement approach that can be applied to low power PV panels stems from the need to optimize shading effects that are common in PV arrays installed inside habitable areas. A first dc/dc buck converter attached to the PV module is controlled through a P&O approach, and a second buck converter is controlled through a polynomial model-based regulator. An electronic implementation on a small PV panel accompanied by a 12 V accumulator validates the results.

Keywords: renewable energy, photovoltaic system, system modeling, polynomial control.

1. Introduction

The advance in research concerning MPPT algorithms is obvious through the many electronic solutions and control methods developed as [4]. Usually buck and boost converters are used, but other solutions are also adopted as the SEPIC [6]. In this work, a consecutive buck configuration is chosen because of its simplicity.

The Buck-Boost structures has been thoroughly analyzed and diverse control solutions have been given as [3]. The article deals with a less used structure that fits well for some cases of high voltage photovoltaic panels connected to lower voltage consumers. The proposed architecture works well for such particular cases, as the generated voltage being high enough will permit the buck converter that deals with the MPPT to reduce the output voltage in an acceptable range.

[1] University Lille 1 Science and Technology of Lille, France, e-mail: arh_cristi@yahoo.com
[2] As. Prof., Faculty of Automatic Control and Computers, University POLITEHNICA of Bucharest, Romania, e-mail: severus.olteanu@acse.pub.ro
[3] Prof., University Lille 1 Science and Technology of Lille, France, e-mail: nicolai.christov@univ-lille.fr
[4] Prof., Faculty of Automatic Control and Computers, University POLITEHNICA of Bucharest, Romania

The interest in the control of individual photovoltaic panels stems not only from the usage of isolated consumers as for example LED based lighting solutions, but also from the perspective of optimizing a large array of panels situated in habitable areas where partial shading cannot be avoided. This is of high interest in current time.

For the MPPT solution itself, a P&O approach is implemented, based on [2]. These solutions are simple to implement numerically and do not require knowledge of the system model. Although they have been well researched and tested in the literature [1],[11],[12], we have chosen such a solution instead of a more complex one like a sliding mode MPPT as in [5] or Takagi-Sugeno one as in [7],[10], because we wanted an as simple to implement algorithm that responds to the industrial demands.

Thus, the paper's contribution comes from the numerical simplicity of the architecture, where the second buck converter is a basic, yet powerful model based polynomial controller; this is important as the two converters influence one another, and a more robust control is in order.

The paper begins by presenting the architecture as a whole, followed by a detailed description of the converters, the MPPT approach and the RST regulator. Finally, results are shown both in simulation and on the hardware test platform, and conclusions are presented.

2. System Architecture

In Fig. 1. The overall system architecture is presented. In the validated scenario, the main load connected to the buck converter is a resistive load (as a heating element or light bulbs). Between the two converters, an auxiliary resistance can be added as well if required (for example for cooling the unit or for local lighting of the system).

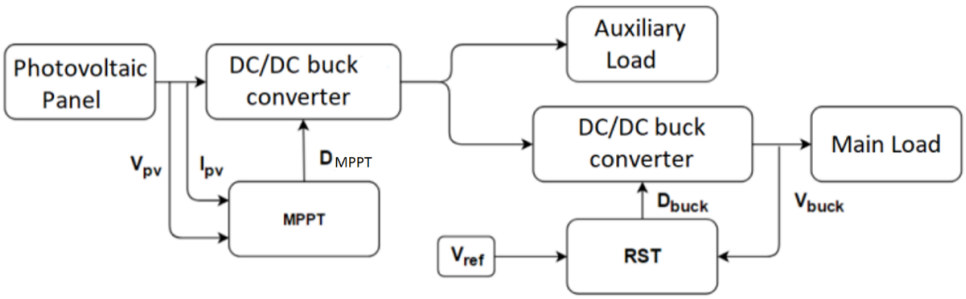

Fig. 1. The overall system architecture

Considering the transistor in the second buck converter, its switching affects the first converter as well, as a continuous variation of the equivalent impedance.

As such, the current oscillates, but its mean value remains constant for a constant input voltage. The buck converters work with an 32Khz frequency command. The inductance value is chosen accordingly, with a value of 160 [µH]. The condensers, at the output we have 220 [µF], and at the input 100 [µF] to smoothen the input.

3. Model based polynomial control

In order to control the output voltage, the dynamical model of the second buck converter has to be developed. The associated transfer function of the process is:

$$H_p(s) = \frac{V}{s^2 L C_b + s\frac{L}{R} + 1} \quad (1)$$

where $L = 160\ [\mu H]$, $C_b = 220\ [\mu F]$ and $V = 22\ [V]$.

The mathematical model of the discretized process is an auto-regressive model with exogenous input (ARX). After using the "zero order hold" discretization method [9] the following discrete transfer function of the model is obtained for a sampling time of 62.5 µs:

$$H_p(z^{-1}) = \frac{z^{-2}(1.151132) + z^{-1}(1.162124)}{z^{-2}(0.971991) + z^{-1}(-1.866843) + 1} \quad (2)$$

A polynomial R-S-T algorithm ([8]) is proposed for controlling the plant model above. The demanded performances are adjusted through some trials simulating the behavior of the global system, including the photovoltaic generator, the converters, variable solar irradiation and temperature.

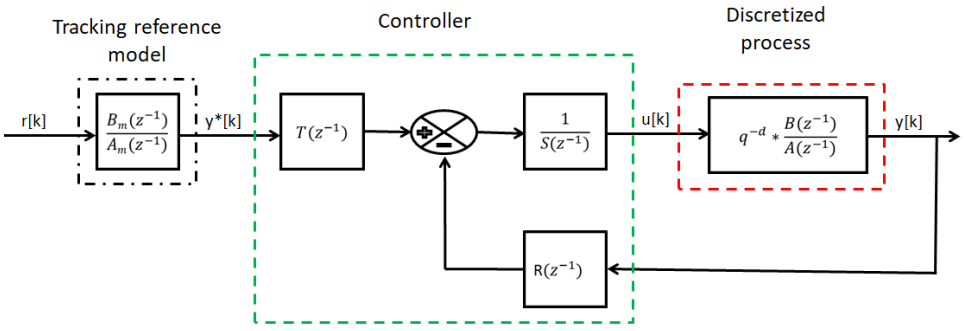

Fig. 2. RST feedback diagram

This control structure takes into account the discretized transfer function of the process, the R-S-T polynomials used for controlling the plant in closed loop and rejecting the disturbances, and the trajectory generator which imposes a desired trajectory. The general RST command form is the following:

$$u(k) = \frac{T(q^{-1})}{S(q^{-1})} r(k) - \frac{R(q^{-1})}{S(q^{-1})} y(k), \qquad \forall\, k \in \mathbb{N} \tag{3}$$

Where the polynomials of the controller are defined as below:

$$\begin{cases} R(z^{-1}) = r_0 + r_1 z^{-1} + \cdots + r_{nr}\, z^{-nr} \\ S(z^{-1}) = 1 + s_1\, z^{-1} + \cdots + s_{ns}\, z^{-ns} \\ T(z^{-1}) = t_0 + t_1\, z^{-1} + \cdots + t_{nt}\, z^{-nt} \end{cases} \tag{4}$$

The polynomials of the plant are defined as below:

$$\begin{cases} B(z^{-1}) = b_1\, z^{-1} + b_2\, z^{-2} + \cdots + b_{nb}\, z^{-nb} \\ A(z^{-1}) = 1 + a_1\, z^{-1} + \cdots + a_{na}\, z^{-na} \end{cases} \tag{5}$$

The coefficients of the plant can be substituted with the values obtained in eq. 2. Further we can compute the transfer function of the closed loop system:

$$H_{cl}(z^{-1}) = \frac{z^{-d}\, T(z^{-1})\, B(z^{-1})}{A(z^{-1})\, S(z^{-1}) + z^{-d}\, B(z^{-1})\, R(z^{-1})} = \frac{z^{-d}\, T(z^{-1})\, B(z^{-1})}{P(z^{-1})} \tag{6}$$

where the poles of the closed loop system are characterized by the polynomial:

$$P(z^{-1}) = p_1 * z^{-1} + p_2 * z^{-2} + \cdots + p_{nb} * z^{-np} \tag{7}$$

The polynomial P contains the dominant and auxiliary poles of the closed loop system:

$$P(z^{-1}) = A(z^{-1})\, S(z^{-1}) + z^{-d}\, B(z^{-1})\, R(z^{-1}) = P_D(z^{-1}) P_F(z^{-1}) \tag{8}$$

$P_D(z^{-1})$ corresponds to the dominant closed loop poles of the system and is responsible with for performances of the controller. $P_F(z^{-1})$ stands for the auxiliary poles of the closed loop system, which are used for filtering purposes, for the improving the robustness of the system. As mentioned in [9], the auxiliary poles are faster than the dominant poles, meaning that the real part of the roots of $P_F(z^{-1})$ is inferior to one of $P_D(z^{-1})$. A second-degree transfer function is used for imposing the dominant poles, thus the desired behavior of the closed loop system; having ζ as the damping factor and ω_0 the natural frequency. Considering the value of the sampling period (62.5 μs), a damping factor $\zeta = 0.8$ and a natural frequency $\omega_0 = 10000$rad/s are chosen. After the discretization we obtain:

$$H_{imposed}(z^{-1}) = 1 - 1.164793 z^{-1} + 0.416862 z^{-2} \tag{9}$$

Then we impose these poles to the polynomial P:

$$P(z^{-1}) = H_{imposed}(z^{-1}) \tag{10}$$

Furthermore, an integrator is added in the *Hs* imposed part of the polynomial *S* in order to obtain a null steady state error.

$$H_S(z^{-1}) = 1 - z^{-1} \tag{11}$$

The coefficients of the R and S polynomials are determined by solving the next equation:

$$x = M^{-1}p \tag{12}$$

where:

$$x^T \stackrel{\text{def}}{=} [1\ s_1\ s_2 \dots\ s_{nb+d}\ r_0\ r_1 \dots\ r_{na-1}]$$
$$p^T \stackrel{\text{def}}{=} [1\ p_1\ p_2 \dots\ p_{na+nb+d}] \tag{13}$$

and $M_{[na+nd+d+1],[na+nb+d+1]}$ is the Sylvester matrix, associated to the coprime polynomials A and B. The values are computed:

$$R(z^{-1}) = 0.228370 - 0.409277z^{-1} + 0.192297z^{-2} \tag{14}$$

$$S(z^{-1}) = 1 - 1.007634z^{-1} + 0.007634z^{-2} \tag{15}$$

The coefficients of the T polynomial are determined from the following expression:

$$T(z^{-1}) = K * P(z^{-1}) \tag{16}$$

where:

$$K(z^{-1}) = \begin{cases} \dfrac{1}{B(1)}, B(1) \neq 0 \\ 1, \quad B(1) = 0 \end{cases} \tag{17}$$

After introducing eq. (18) in (17) we obtain:

$$T(z^{-1}) = 0.432291 - 1.127883\ z^{-1} + 1.144695\ z^{-2} - 0.536612\ z^{-3} + 0.098899z^{-4}$$

The transfer function of the tracking reference model is:

$$H_m(z^{-1}) = \frac{z^{-1}\ B_m(z^{-1})}{A_m(z^{-1})} = \frac{z^{-1}\ (b_{m1} + b_{m2}\ z^{-1})}{1 + a_{m1}z^{-1} + a_{m2}\ z^{-2}} \tag{19}$$

To obtain the polynomials *Am* and *Bm* of the trajectory generator, another transfer function of second degree is used. A damping factor $\zeta = 0.8$ and a natural frequency $\omega_0 = 12000$rad/s are chosen. The same procedure is applied as for computing the polynomials *R* and *S*.

$$B_m(z^{-1}) = 095495\ z^{-1} + 0.073072z^{-2} \tag{20}$$

$$A_m(z^{-1}) = 1 - 1.280762\ z^{-1} + 0.449329\ z^{-2} \tag{21}$$

After obtaining all the parameters of the above-mentioned polynomials the performances of the control algorithm are tested in simulation, as shown in Fig. 3.

The control loop is tested on the model of the DC/DC buck converter in Matlab-Simulink. During the simulation, two types of disturbances are being

applied to the control loop. After the reference is reached, the element of execution, the transistor from the Sziklai pair, is being disconnected from the controller. Later on, an additive disturbance is applied to the control law. We can observe that in Fig. 3 that the MPPT control algorithm is harvesting the maximum power that the PV can provide, with respect to the second control loop which perturbs it as well.

Furthermore, we can observe the two types of disturbances proposed earlier. The first one which is triggered during the time interval [0.4s, 0.41s] is not well rejected, because the control law is saturated at maximum value, while the static error is superior to 13.3%. The second one which is triggered during the time interval [0.8s, 0.85s] is well rejected.

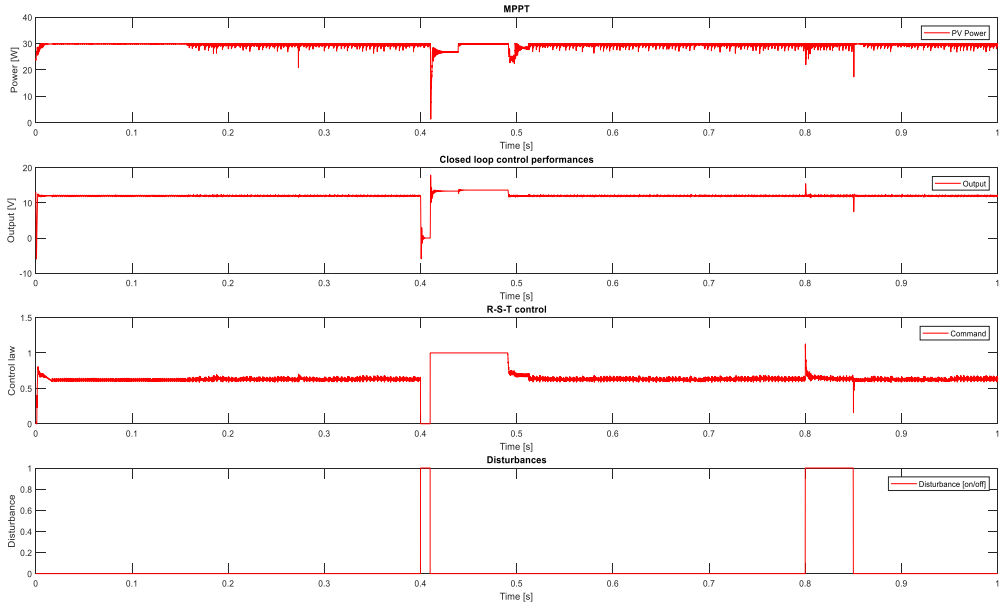

Fig. 3. Closed loop control with the R-S-T control polynomial

4. Robust RST control algorithm

An output sensitivity functions is used to analyze the performances of the controller:

$$S_{yp}(z^{-1}) = \frac{A(z^{-1}) * S(z^{-1})}{A(z^{-1}) * S(z^{-1}) + z^{-d} * B(z^{-1}) * R(z^{-1})} \tag{22}$$

We shall consider the margin modulus:

$$\Delta M \stackrel{\text{def}}{=} \min_{\omega \in R} \left|1 + H\left(e^{j\omega}\right)\right| \tag{23}$$

$$\Delta M|_{db} = -\max_{\omega \in R} |S_{yp}(e^{j\omega})|\Big|_{db} \tag{24}$$

A bigger value of ΔM implies a better robustness. In order to achieve it, the value of *Syp* must decrease.

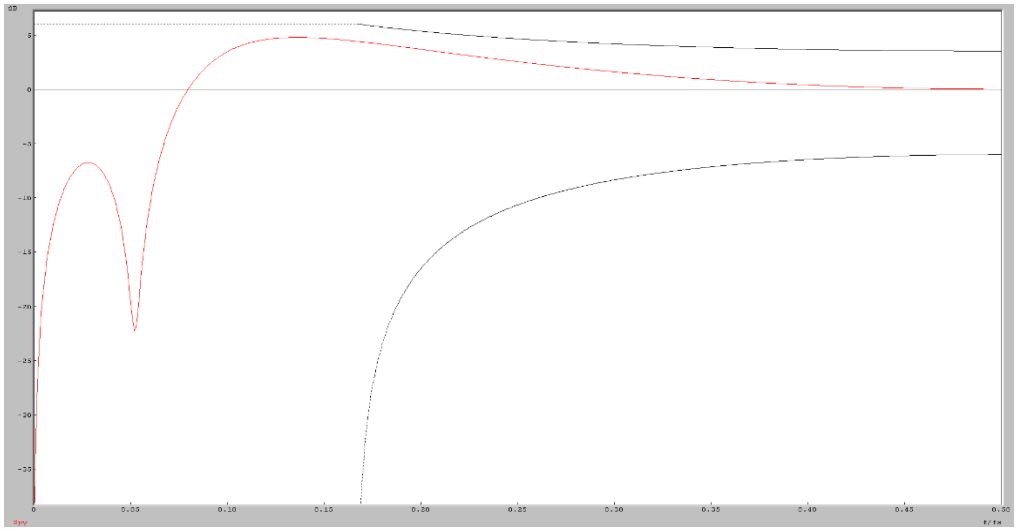

Fig. 4. Sensitivity function – Syp (R-S-T)

In the Fig. 4. is presented the sensitivity function *Syp*. After computing with the WinReg Robustness Analysis routine we obtain $\Delta M = -4.78$ dB. The performances in regulation and tracking can be improved tracking by introducing auxiliary pairs of poles/zeros and/or introducing pre-specifications for the *R* and *S* polynomials.

Next, we shall create a robust R-S-T polynomial controller. An extra pair of complex poles to the tracking, imposing another second-degree transfer function with a damping factor $\zeta = 0.8$ and a natural frequency $\omega_0 = 6000$rad/s. Poles and zeros of the system can be pre-specified in the polynomial H_S and H_R as presented below:

$$S = H_S * S'; R = H_R * R' \tag{25}$$

The following poles will be imposed:

$$H_S(z^{-1}) = (1 - z^{-1})(1 - 0.2z^{-1})(1 - 0.4z^{-1})(1 - 0.15z^{-1}) \tag{26}$$

The values of all the polynomial are recomputed:

$$R(z^{-1}) = 0.456929 - 1.129520z^{-1} + 1.032453z^{-2} - 0.420929z^{-3} + 0.077288z^{-4} - 0.004831z^{-5}$$

$$S(z^{-1}) = 1 - 1.273248z^{-1} + 0.085684z^{-2} + 0.256612z^{-3} - 0.074769z^{-4} + 0.005721z^{-5}$$

$$T(z^{-1}) = 0.432291 - 1.127883z^{-1} + 1.144695z^{-2} - 0.536612z^{-3} + 0.098899z^{-4}$$

$$B_m(z^{-1}) = 0.095495 + 0.073072z^{-1}$$

$$A_m(z^{-1}) = 1 - 1.280762z^{-1} + 0.449329\,z^{-2}$$

As for the first RST computed controller, the closed loop control is tested in WinReg software for reference tracking and rejection of the disturbance for both robust and standard controllers. A slight improvement related to the rejection of the disturbances, with the tradeoff of having a higher amplitude of the control signal. Next, we shall analyze the sensitivity functions of the two controllers, as presented in Fig. 5.

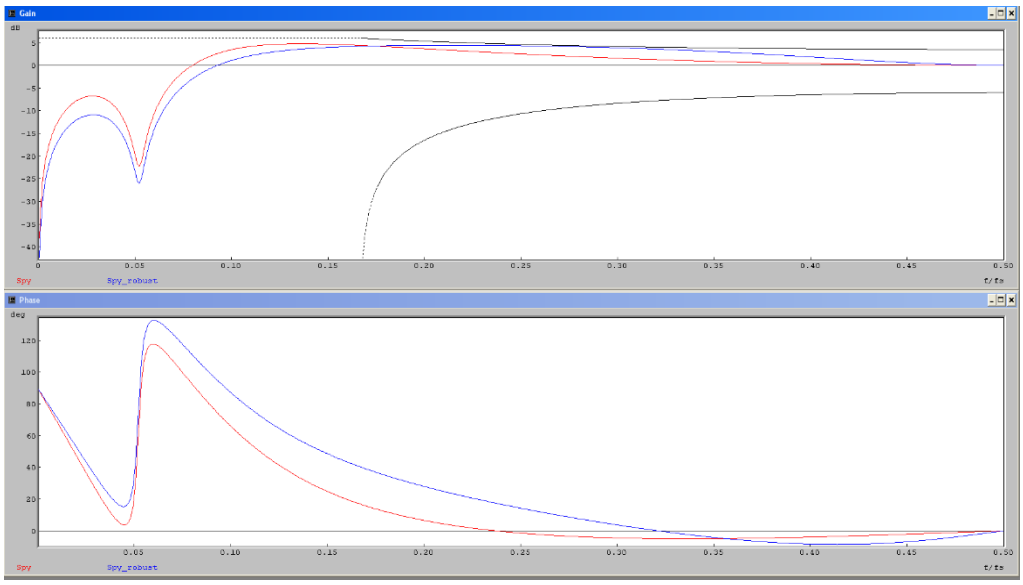

Fig. 5. Sensitivity functions – Syp (R-S-T) of robust controller vs standard controller

An improved value of $\Delta M = -4.44\ dB$ is obtained. Then, the control loop is tested on the model of the DC/DC buck converter, as presented in the figure below. We can observe in Fig. 6 that the rejection of both types of disturbances is slightly improved.

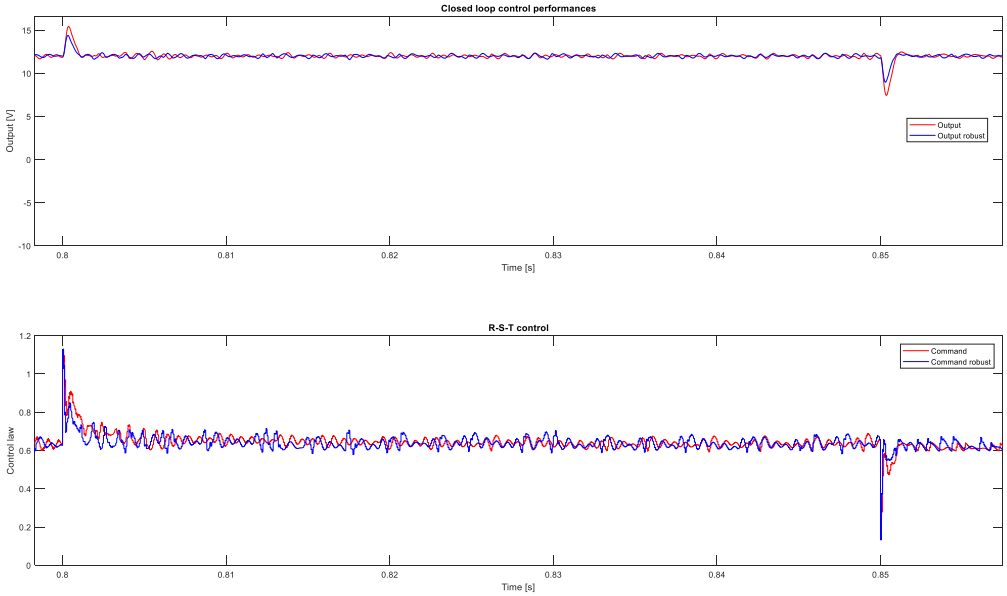

Fig. 6. Rejection of disturbances (scenario II) – robust vs. standard RST

5. Robust RST control system with anti-windup

During the first type of perturbation we can observe that the command is saturated. Therefore, an anti-windup technique can be used to avoid this kind of scenarios.

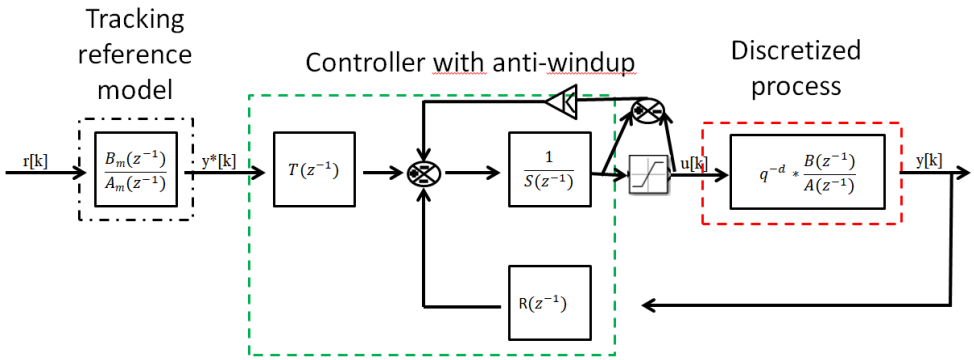

Fig. 7. RST feedback diagram with anti-windup

The error between the control law generated by the controller and its value after the saturation block can be multiplied with a gain and be reintroduced in the control loop, as presented in Fig. 7. The new controller is tested within the same conditions. The results presented in Fig. 8 confirm us that the new control law is

improved. The command is not saturated anymore in the first testing scenario, aspect which leads to a fast rejection of the disturbance.

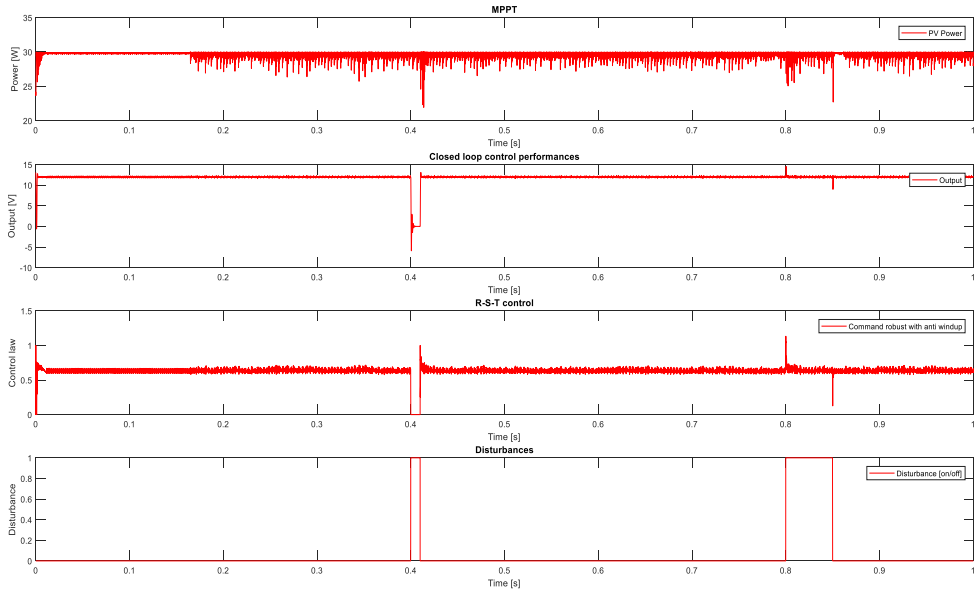

Fig. 8. Closed loop control with the robust R-S-T control polynomial with anti-windup

In Fig. 9 is described the implementation of the DC/DC step down converter.

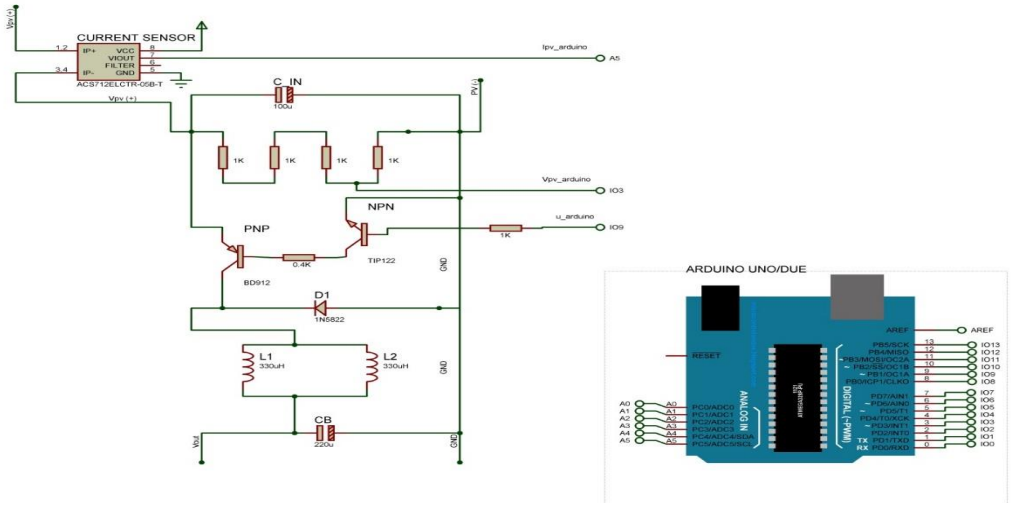

Fig. 9. Hardware implementation DC/DC

The Arduino Uno measures the voltage of the panel delivered via a voltage divider circuit, and the current of the panel provided by a Hall effect current sensor. It controls the DC/DC converter via a 32Kh frequency output pin which is connected to a Sziklai pair or complementary Darlington. For the achieving the imposed performances a loop that runs at a frequency of 16kHz was used. First the code was run on an Arduino Uno architecture. The frequency of the control loop was limited to maximum 3kHz.

The performances of the regulator were not satisfactory if the output was measured with an oscilloscope. Therefore, a change of architecture was required, which lead to the use of Arduino Due. The obtained results are presented in Fig. 10. The reference of 12V for charging the battery is well tracked by the controller.

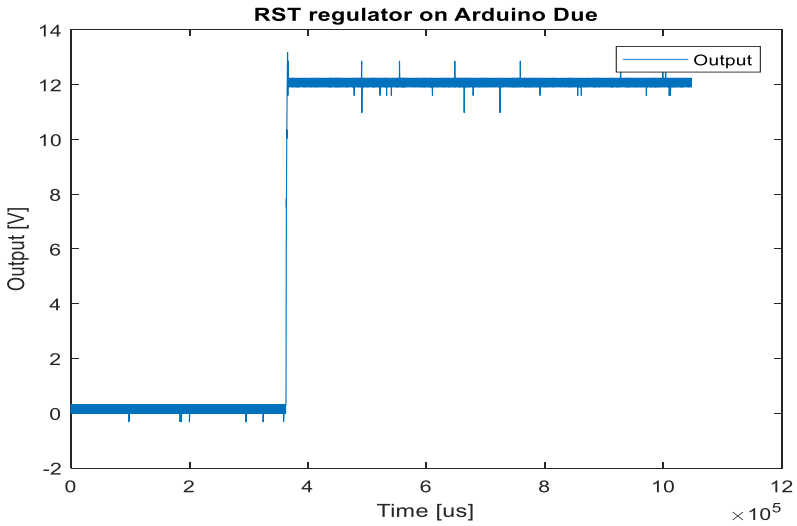

Fig. 10. Implementation of RST controller on Arduino Due

There are some spikes in measurement data, because of the really high resolution that was used to measure with the oscilloscope.

6. Conclusions

This paper dealt with the design of an architecture for the optimal usage of photovoltaic energy.

The approach is based on a Buck converter configuration, where the first converter is controlled through an improved P&O approach, whereas the second converter is controlled through a polynomial RST algorithm that needed to be robust enough to reject perturbations risen from the influence of the MPPT converter. The solution is well suited for high voltage PV panel arrays, offering an un-expensive solution that can be easily reproduced for all PV modules.

The solution was validated in an electrical simulation on a small photovoltaic panel giving good results. As a perspective, this approach is to be improved with better control algorithms for the MPPT part, as the P&O is not the best solution.

The sampling period has been chosen in an optimal way in order to be large enough to be simple in its numerical implementation yet small enough to give good results. The sampling period, for reading the sensors and converting the values to numerical format, needs to be fast enough, considering the 30Khz PWM frequency.

R E F E R E N C E S

[1] *T. Murali Mohan and V. Vakula*. „Comparative analysis of perturb & observe and fuzzy logic maximum power point tracking techniques for a photovoltaic array under partial shading conditions“, in Leonardo Journal of Sciences **Vol. 27** (2015), pp. 1–16.

[2] *C. Miron, N. Christov, and S. C. Olteanu*, „Energy management of photovoltaic systems using fuel cells “. In: System Theory, Control and Computing (ICSTCC), 2016 20th International Conference on. IEEE. 2016, pp. 749–754.

[3] *B. J. Saharia, M. Manas and S. Sen*, "Comparative Study on Buck and Buck-Boost DC-DC Converters for MPP Tracking for Photovoltaic Power Systems," 2016 Second International Conference on Computational Intelligence & Communication Technology (CICT), Ghaziabad, 2016, pp. 382-387.

[4] *M. A. Eltawil, Z. Zhao*, “MPPT Techniques for Photovoltaic Applications”, Renewable and Sustainable Energy Reviews, **Vol. 25**, 2013, pp. 793-813.

[5] *A. Belkaid, J. P. Gaubert, A. Gherbi and L. Rahmani*, "Maximum Power Point tracking for photovoltaic systems with boost converter sliding mode control," 2014 IEEE 23rd International Symposium on Industrial Electronics (ISIE), Istanbul, 2014, pp. 556-561.

[6] *R. B. Darla*, "Development of maximum power point tracker for PV panels using SEPIC converter," INTELEC 07 - 29th International Telecommunications Energy Conference, Rome, 2007, pp. 650-655.

[7] *C. S. Chiu*, “TS Fuzzy Maximum Power Point Tracking Control of Solar Power Generation Systems”, IEEE Transaction on Energy Conversion, 2010.

[8] *Dimon C., Geneviève D.T., Popescu D., Tache I.A.* – “Numerical Control for Hydrodynamic Traffic Flow Models”, 1st International Conference on Systems and Computer Science (ICSCS 2012), France, August 2012.

[9] *D. Popescu, A. Gharbi, D. Stefanoiu, P. Borne*, Process Control Design for Industrial Applications (Systems and Industrial Engineering - Robotics), ISBN-13: 978-1786300140, 2017.

[10] *C. Miron, D. Popescu,A. Aitouche and N. Christov*, “Observer based control for a PV system modeled by a Fuzzy Takagi Sugeno model”, in 2015 System Theory, Control and Computing (ICSTCC), 2015 19th International Conference, pp. 652-657, 2015.

[11] *M. Kaouane, A. Boukhelifa, A. Cheriti*, Regulated output voltage double switch Buck-Boost converter for photovoltaic energy application, International Journal of Hydrogen Energy, **Vol. 41**, Issue 45, Pages 20847-20857, ISSN 0360-3199, 2016.

[12] *Mihai IONESCU* P&O maximum power point regulation model for two stage grid connected pv systems, U.P.B. Sci. Bull., Series C, Vol. 80, Iss. 2, 2018